A new method for pedicel/peduncle detection and size assessment of grapevine berries and other fruits by image analysis

S. Cubero[1,2], M.P. Diago[2,3], J. Blasco[1], J. Tardaguila[2], B. Millán[2], N. Aleixos[4*]

[1]Centro de Agroingeniería. Instituto Valenciano de Investigaciones Agrarias (IVIA). Cra. Moncada-Náquera km 5, 46113 Moncada (Valencia), Spain.

[2]Instituto de Ciencias de la Vid y del Vino (University of La Rioja, CSIC, Gobierno de La Rioja). 26006 Logroño. Spain.

[3]Università Cattolica del Sacro Cuore, Via Emilia Parmense 84, 29122, Piacenza, Italia.

[4]Instituto Interuniversitario de Investigación en Bioingeniería y Tecnología Orientada al Ser Humano. Universitat Politècnica de València. Camino de Vera s/n, 46022 Valencia, Spain. Email: naleixos@dig.upv.es

Abstract

The berry size of wine-grapes has often been considered to influence wine composition and quality, as it is related to the skin-to-pulp ratio of the berry and the concentration of skin-located compounds that play a key role in the wine quality. The size and weight of wine-grapes are usually measured by hand, making it a slow, tedious and inaccurate process. This paper focuses on two main objectives aimed at automating this process using image analysis: 1) to develop a fast and accurate method for detecting and removing the pedicel in images of berries, and 2) to accurately determine the size and weight of the berry. A method to detect the peduncle of fruits is presented based on a novel signature of the contour. This method has been developed specifically for grapevine berries, and later extended and tested with an independent set of other fruits with different shapes and sizes such as peppers, pears, apples or mandarins. Using this approach, the system has been capable of correctly estimating the berry weight (R2>0.96) and size (R2>0.97) of wine-grapes and of assessing the size of other fruits like mandarins, apples, pears and red peppers (R2>0.93). The proven performance of the image analysis

methodology developed may be easily implemented in automated inspection systems to accurately estimate the weight of a wide range of fruits including wine-grapes. In this case, the implementation of this system on sorting tables after de-stemming may provide the winemaker with very useful information about the potential quality of the wine.

Keywords: Image analysis; Contour function; Pedicel detection; Grape berries, Size and weight estimation

1. Introduction

Machine vision systems are being used to automate inspection tasks in agriculture and food processing. Apart from its use in defect detection or colour estimation, image analysis is also an objective and reliable tool for examining other features such as shape and size (Cubero et al., 2011; Lorente et al., 2012).

Berry size and weight are two key parameters in the quality of table and wine-grapes. Berry size and weight parameters not only have an impact on the cluster architecture and compactness (leading to looser or tighter clusters), thereby influencing the cluster health status (Tardaguila et al., 2010), but are also considered indicators of grape and wine quality. In fact, berry weight and size, and their implications in grape and wine quality, have been extensively studied worldwide (Roby et al., 2004; Walker et al., 2005) and recently reviewed by Matthews and Nuzzo (2007). Most of the key compounds for wine quality, such as aromas and phenols, are located in the skin (Kennedy, 2010). Therefore, it is widely assumed that better wines are made from smaller berries, which have higher skin-to-pulp ratios (Barbagallo et al., 2011). Berry weight and size are common parameters for assessing wine-grapes' ripening from veraison to harvest (Iland et al., 2004) and quality features in table grapes. Their assessment – usually performed in the laboratory – often requires the removal of the berry pedicel, which is time and labour consuming.

Image analysis has recently been used outdoors to characterise several grapevine features, such as leaf area and yield (Diago et al., 2012). An important step forward would be the capacity to estimate berry size and weight from the analysis of images taken in the field, i.e. of the clusters hanging on the vines. This would allow close non-destructive monitoring of berry size throughout the ripening period of the actual clusters. In this respect, the detection of berry pedicels would be an even more critical step to avoid confounding effects.

The automatic detection of the pedicel in berries, or peduncle in other fruits (pedicel is normally used in the case of grain fruits that are joined together in a bunch and peduncle is more common for fruits joined directly to the branch of the plant), is still a challenge. Kapach et al. (2012) offered an extensive description of the computer vision techniques that can be used for fruit-harvesting robots, concluding that the automation of some specific tasks is especially difficult, such as the detection of the peduncle in the grasping and picking operations carried out by the robot.

In some fruit, like oranges, the presence of large peduncles can damage other fruits during storage but their absence is considered a loss of quality. Sometimes it is important to detect the peduncle clearly in order to avoid confounding effects between the presence of the peduncle and external damage in automated quality inspection systems. If the peduncle is visibly different from the fruit, strategies based on colour information can be applied to locate it. Laykin et al. (2002) used colour information to discriminate between the peduncle on tomatoes and bruises with a success rate of 100%. However, in other cases the difference between the peduncle and other defects is not so apparent. In these situations, Blasco et al. (2007) used visible images complemented by a multispectral system to discriminate among the peduncle and various defects in citrus fruits, achieving a peduncle identification rate of 67%.

Peduncle detection is also needed when information regarding the orientation of the fruit is required. Bennedsen and Peterson (2005) developed a computer vision system to detect defects in apples that had previously been oriented towards preventing the peduncles from appearing in the image. For the orientation process, these authors used a prototype developed by Throop et al. (2003), who oriented the apples with the peduncle on one side. In another work, Lu and Peng (2006) needed the fruit to be

78 oriented with the end of the peduncle horizontal in order to obtain scattering measures in peaches. A
79 similar idea was used by Blasco et al. (2003), who acquired four images of apples from different views
80 in order to estimate the size of the fruit in the image based on the equatorial diameter. For this
81 purpose, the more perpendicular and centred the peduncle was, the better.

82 Harvesting robotics may also require peduncle detection systems to be implemented in order to collect
83 the fruit properly. In this regard, Van Henten et al. (2006) presented a robotic system for de-leafing
84 cucumber plants. To perform its tasks, the robot identified the pedicel of each leaf using two images at
85 wavelengths of 850 nm and 970 nm, which can potentially be exported for use in actual harvesting
86 robots. Hayashi et al. (2010 and 2011) used a machine vision unit based on three cameras installed on
87 a robotic harvesting system to detect the position of strawberries and the orientation of the peduncle,
88 thereby allowing accurate guidance of the robotic arm.

89 As can be seen, the detection of fruit peduncles is an important issue to be taken into account in the
90 design of a computer vision system for estimating the quality features of fruit or vegetables. Several
91 solutions have been proposed to determine the peduncle position, such as: the use of structured
92 lighting to detect concavities in apples (Yang, 1993); colour segmentation techniques to differentiate
93 the calyx and peduncle in citrus fruits (Ruiz et al., 1996); or the study of light reflection in apples
94 (Penman, 2002). In some of these works, the use of a spectral imaging system to locate the peduncle
95 and discriminate it from other damage was required. Thus, the peduncles of some fruits present
96 different reflectance values in the NIR region in relation to the skin of the fruit at certain wavelengths.
97 Xing et al. (2007) used the texture of multispectral images to discriminate between smooth faces and
98 those presenting peduncles in apples of different colours. A similar approach was taken by Nanyam et
99 al. (2012) to detect and discriminate the peduncle and leaves from defects in strawberries.

100 The main objective of this work was to develop an effective new method using image analysis and
101 based on contour signatures to detect and remove the pedicel in images of grapevine berries using
102 machine vision, and thus accurately determine the weight and size (diameter) of grape berries. The
103 algorithm was also tested with other fruits like mandarins, apples, pears, and so on to validate it.

This paper is organised as follows. In section 2 we present the materials and methods, including a description of the plant material, the vision system, the segmentation process and a detailed description of the peduncle/pedicel location algorithm. In section 3 we present the results obtained for the size and weight of grape berries, including the results for other fruits to validate the algorithm, as well as some discussion of the results. Finally, section 4 offers some conclusions from this work.

2. Materials and methods

The algorithms were developed and tuned using different images of 20 wine-grape berries of several colours and sizes, and captured with the pedicel at various random orientations. They were validated using another independent set of 100 single berries of different sizes and colours belonging to two grapevine (*Vitis vinifera* L.) cultivars (50 samples of Grenache and 50 of Tempranillo). The berries were placed on a white background inside a chamber equipped with a still camera (EOS 550D, Canon Inc, Japan) and four lamps each containing two fluorescent tubes (Osram L 18W/965 BIOLUX) with a colour temperature of 6500 ºK. The angle between the axis of the lens and the sources of illumination was approximately 45º, the insides of the inspection chamber were coated with anti-reflective material, and cross-polarisation was achieved by placing polarising filters in front of the lamps and in the camera lenses to minimise the impact of specular reflections produced on spherical fruits. The berries were oriented with the pedicel facing upwards and downwards interchangeably and the images were obtained with a size of 2592 x 1944 pixels and a resolution of 0.11 mm/pixel. The berries in the images included the pedicel, which makes it necessary to detect the insertion point between the fruit and the pedicel in order to obtain accurate measurements of the berry parameters. Two algorithms based on the radius function (Kunttu and Lepisto, 2007) and arc-length versus the turning angle graph (Wolfson, 1990) of the contour were developed to detect these points in the contour of the objects found in the images. In addition, a new algorithm based on a signature derived from these previous functions is proposed to improve the performance and robustness of a potential automatic system. To make the algorithm more robust and potentially general, the algorithms were also tested in other fruits

like mandarins, pears, apples and peppers representing bigger spherical fruits, non-spherical fruits and irregular fruits with different types of peduncles and with randomly oriented peduncles.

For the manual assessment of grape berry size and weight, all imaged grape berries were individually labelled and weighed (XR205SM-DR, Precisa Instruments Ltd., Switzerland), and their size was measured manually using an electronic calliper (Digitcal, TESA SA, Switzerland) to determine the peduncle/pedicel-calyx (stem-calyx) axis and equatorial diameters. The resolution used for the size measurements was 0.01 mm. For the rest of the fruits tested to validate the peduncle/pedicel location algorithm, all the manual measurements for determining the stem-calyx axis and the equatorial diameters were carried out using the same electronic calliper.

2.1. Segmentation and contour detection processes

Prior to the segmentation of images, an off-line process is carried out. This process consists in generating a look-up table (LUT) that is later used to segment the images of the fruit. This process is performed using a computer application specially developed for this purpose that allows an operator to select different windows in the images representing the background and peel/stem classes. The RGB values of the training windows selected are used as input in a Bayesian discriminant model (Harrel, 1991), the independent variables of the model thus being the grey levels of the RGB bands. Finally, the model is stored in an LUT which contains the classes of the model, and thus the segmented image contains the classes that each pixel belongs to. After image segmentation, a binary image showing the fruit in white and the background in black was obtained. The next step was to apply an algorithm which extracted the eight-connected contour by means of the chain code described by Freeman (1961).

2.2. Peduncle/pedicel location algorithm

One of the key points of the methodology presented here was the algorithm proposed to detect the connecting points between the peduncle and the fruit by analysing the contour of the fruit. Several approaches to analysing the contour of the objects have already been proposed for different purposes, like the analysis of the shape. Many of them propose the use of signatures, which are methods that represent a contour using a one-dimensional function. The best known is probably the radius signature

(Blasco et al., 2009; ElMasry et al., 2012), which can yield a useful description of the shape of regular or manufactured objects with a known shape, but could fail when it is applied to biological objects with irregular or different shapes. Signatures are invariant against size or orientation, which makes them particularly interesting in cases where the size or the orientation of the object is unknown. Applied to peduncle detection, the main problem appears in irregular fruits, which present large variations in their signatures that make them unsuitable to identify the peduncle properly. Even in regular-shaped fruits this signature is sometimes not robust enough to ensure good results. A different descriptor of the perimeter is the curvature signature, although it has not been used frequently for food analysis but is common in other fields (Guliato et al., 2008). Both of them have been tested in this work. The approach proposed in the present study was to obtain a new signature derived from the radius signature. This new signature analyses the changes in the direction of the curvature of the radius function. In regular fruits, these changes are supposed to be very smooth except when peduncle exists.

In the berries, the detection of the pedicel was carried out by an algorithm that consists in the following steps:

1. The centre of mass of the berry was calculated as the average coordinates of the pixels belonging to the fruit. A faster method that could be used instead when the processing time is a constraint would involve using only the information about the boundary to estimate the centroid of the fruit. But in this case, the centroid could be too biased towards the pedicel/peduncle location if it is too long, and the performance of the method could decrease.

2. The radius function (Rubine, 1991) of the berry contour was calculated as a one-dimensional function in which each item of data was the Euclidean distance between the centroid and each of the points on the contour. This is represented in Figure 1, where Figure 1a shows a sample of the original image of a berry and the contour extracted with its centroid position. The radius function is shown in Figure 1b. In this function it is supposed that the farthest point from the centroid corresponds to the top of the pedicel/peduncle and therefore the two local minima around this point are selected as the connecting points between the pedicel/peduncle and the

fruit. The maximum value of the radius signature for the end of the pedicel/peduncle (1) and the two contact points of the pedicel/peduncle with the berry (2), (3) can also be observed.

3. The second function calculated was based on the arc-length versus the turning angle graph of the curvature (Kalvin et al., 1986). In essence, the curvature consists in the rate of change of θ, the angle between the tangent vector to the curvature, and the horizontal axis for each point in the contour. The present work made use of the turning angle function (also called direction function), which consists in the graph showing the difference in θ at equally spaced points in the contour S_i ($i=1..n$), the difference being computed as reflected in equation (1) (Shih, 2010):

$$\Delta\theta(S_i) = \theta(S_i+\Delta S)-\theta(S_i) \quad (1)$$

In this work ΔS was set to 4, which was enough to capture changes in the direction of the contour. Therefore, the equation (1) was modified as follows:

$$\Delta\theta(S_i) = \theta(S_{i-2})-\theta(S_{i+2}) \quad (2)$$

For regular curves or shapes, the arc-length versus turning angle graph should be a monotonic decreasing function with values in the interval $[-\pi, +\pi]$ radians. When changes in the contour are encountered due to irregular shapes or the presence of pedicel/peduncle, these are reflected on the graph of the function and can therefore be detected and analysed. An example of this signature is also shown in Figure 1b for a berry with the pedicel oriented downwards.

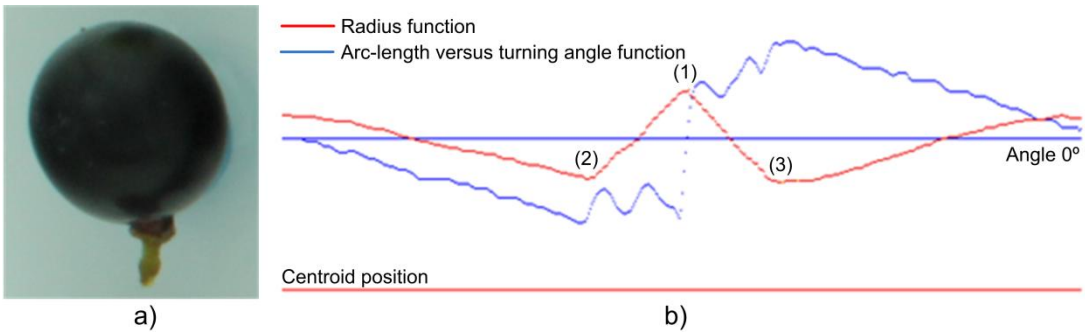

FIGURE 1. a) Original image and contour of a grape berry with pedicel; and b) its corresponding radius function and arc-length versus turning angle function

4. Finally, both functions were mixed to obtain a new one derived from the radius function that was thereafter called the radius direction signature. The new function was then obtained by applying the arc-length versus turning angle using the radius function as input instead of the fruit contour, which allows drastic changes in the outline of the fruits to be detected. This new function took values close to zero when the radius signature presented small changes, and different from zero otherwise.

Under the premise that the contour moves away from the centroid in the pedicel/peduncle part (the distance between the contour and the centroid increases), this new signature attempted to detect the points where these changes in the direction happened. In the case of spherical fruits, the distance from the contour to the centroid should be very similar for all points on the contour and therefore the function should present small changes. In a similar way, in the case of elliptical or other regular-shaped fruits, the changes should be smooth and constant. Figure 2 shows several samples of berries with different orientations of the pedicel (Figure 2a) and their corresponding signatures (Figure 2b). The local maximums have been centred in the graphs to make them easier to understand.

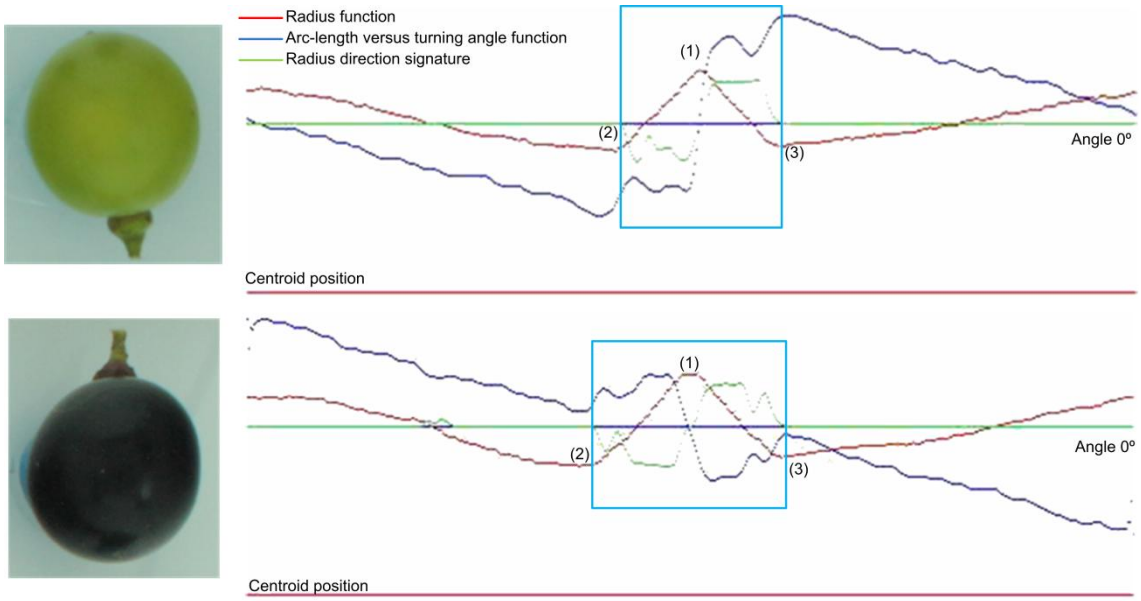

a) b)

220 FIGURE 2. a) Two samples of grape berries; and b) their corresponding radius and arc-length versus
221 turning angle function and radius direction signature

222

223 2.3. Validation process in grape berries

224 To estimate berry size, each individual berry was first located in the image and then the pedicel was
225 detected following the algorithm described above. The two points identified as the connecting points
226 between the pedicel and the fruit were joined to close the fruit contour while excluding the pedicel.
227 Then, the centroid was calculated again without the influence of the pedicel and the size was estimated
228 by means of the peduncle/pedicel axis and the diameter crossing the centroid, which was
229 perpendicular to the previous peduncle/pedicel axis (equatorial diameter). The area of each berry was
230 also estimated as the number of pixels belonging to the fruit excluding the pedicel. The information
231 about the area was used to predict the weight of each individual berry. The flowchart of the features
232 extraction algorithm can be found in Figure 3 and the pseudo-code of the main algorithm is presented
233 in Figure 4.

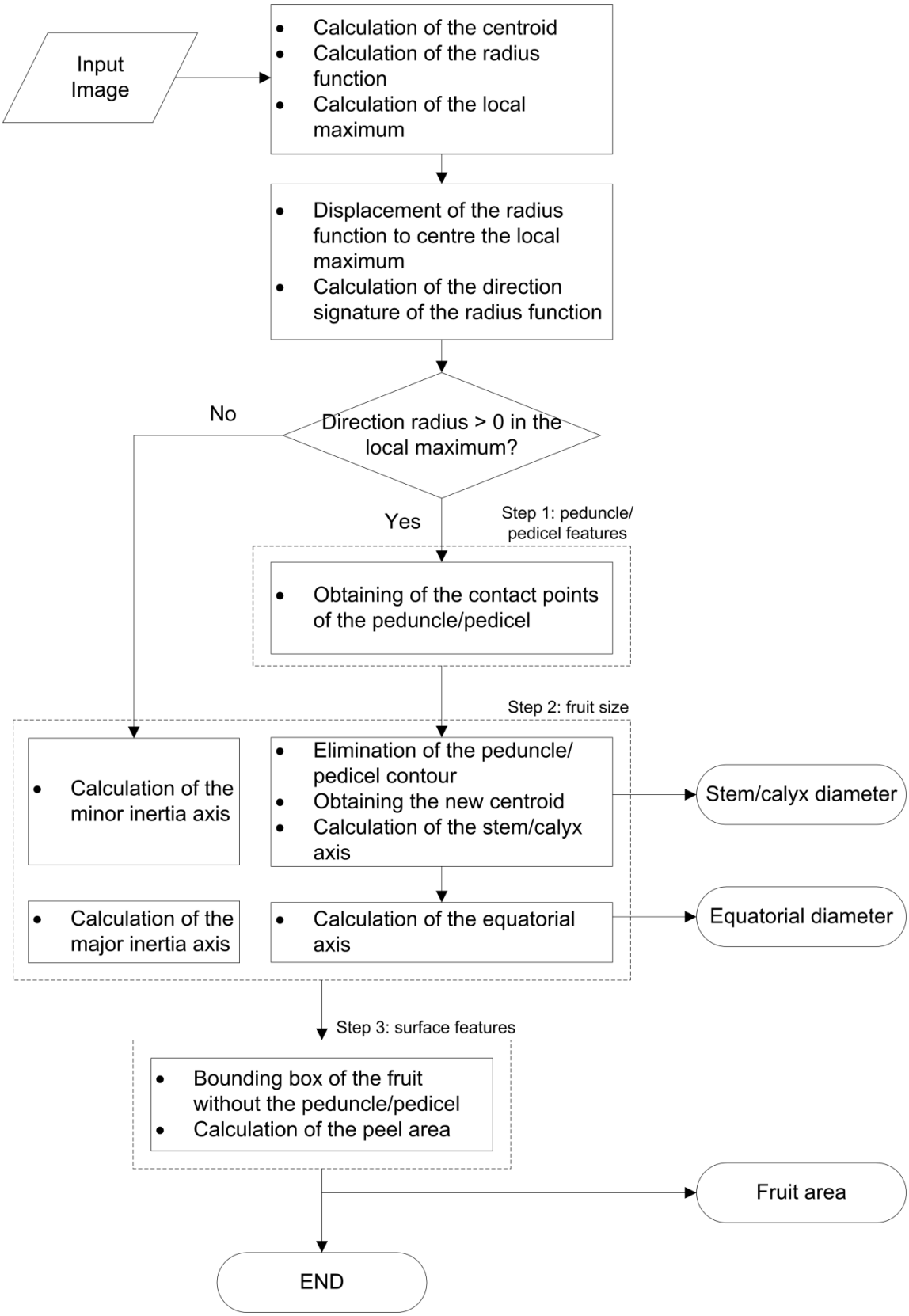

234

235 FIGURE 3. Flowchart for peduncle/pedicel detection and features extraction

```
main () {

        Calculate the Radius_function of the contour;
        Search for the Maximum value in the Radius_function;
        Shift the contour so that the element corresponding to the Maximum in
            the Radius_function is centred;

        Calculate the Radius_function_new of the shifted contour;

        Calculate the Direction_function as the Arc-length versus the turning
            angle graph of the curvature;

        Calculate the Direction_Radius_function as the Arc-length versus the
            turning angle graph of the Direction_function;

        peduncle = false;
        for (i=0; i<total_points_contour; i++)
               if (Radius_Direction_function[i] != 0.0) {
                         peduncle = true;
                     break;
                   }
         if (peduncle) {
               Search for the Local_minimum_1:
                  for (i=0; i<total_points_contour/2; i++)
                             if (Radius_Direction_function[i] != 0.0) {
                                          Local_minimum_1 = i; break;
                             }
               Search for the Local_minimum_2:
                  for (i=total_points_contour; i>total_points_contour/2; i--)
                             if (Radius_Direction_function[i] != 0.0) {
                                          Local_minimum_2 = i; break;
                             }
                  Recalculate centroid without peduncle contour points;
                  Remove peduncle contour points from original contour;
                  fruit_size:
                      Calculate stem/calyx diameter;
                          Calculate equatorial diameter;
                  fruit_weight = Calculate fruit_area;

         }
         else {
                  fruit_size   = Calculate inertia axes;
                  fruit_weight = Calculate total_area;
         }
}
```

FIGURE 4. Pseudo-code of the algorithm for peduncle/pedicel detection

In order to assess the performance of the imaging system developed to predict the size (polar diameter) and weight of the berries in images including the pedicels, a regression model was built on a training set of 66 of the 100 berries. The remaining 34 berries were later used for validation.

2.4. Validation process in other fruits

To test the performance and robustness of the algorithm as well as its capability to be generalised to other fruits, a number of types of fruit with different shapes, sizes and colours were imaged in a variety of orientations and the images were processed to find the peduncles and size using the proposed approach. Particularly, a total of 30 pieces of each of these sets of fruits were used: pears cv. 'Blanquilla', apples cv. 'Golden Delicious' and cv. 'Royal Gala', red bell peppers cv. 'Lamuyo', and mandarins cv. 'Nova'. For each set of different fruits, the peduncle was visible in the image for a total of 25 out of 30 fruits. The rest of the fruit had no peduncle or it was located inside the projected area of the fruit. In the case of red peppers, all the samples contained peduncle. The size of this set was measured manually along the peduncle axis using a digital calliper and the measurements were recorded. The size of all the fruits was also estimated as the peduncle diameter from the closed contour of the fruit, excluding the peduncle.

Some of the results of the peduncle location algorithm for the fruits tested in this work are shown in Figure 5. The points of contact between the peduncle and the fruit are depicted by small yellow and blue key points (small squares), and the base point of the peduncle is the midpoint in-between (pink key point). The distance between the base point of the peduncle and its opposite key point represents the diameter of the peduncle/pedicel, and the other two points on both sides of the centroid determine the length of the equatorial axis, both of which later correlated with the calliper measurements.

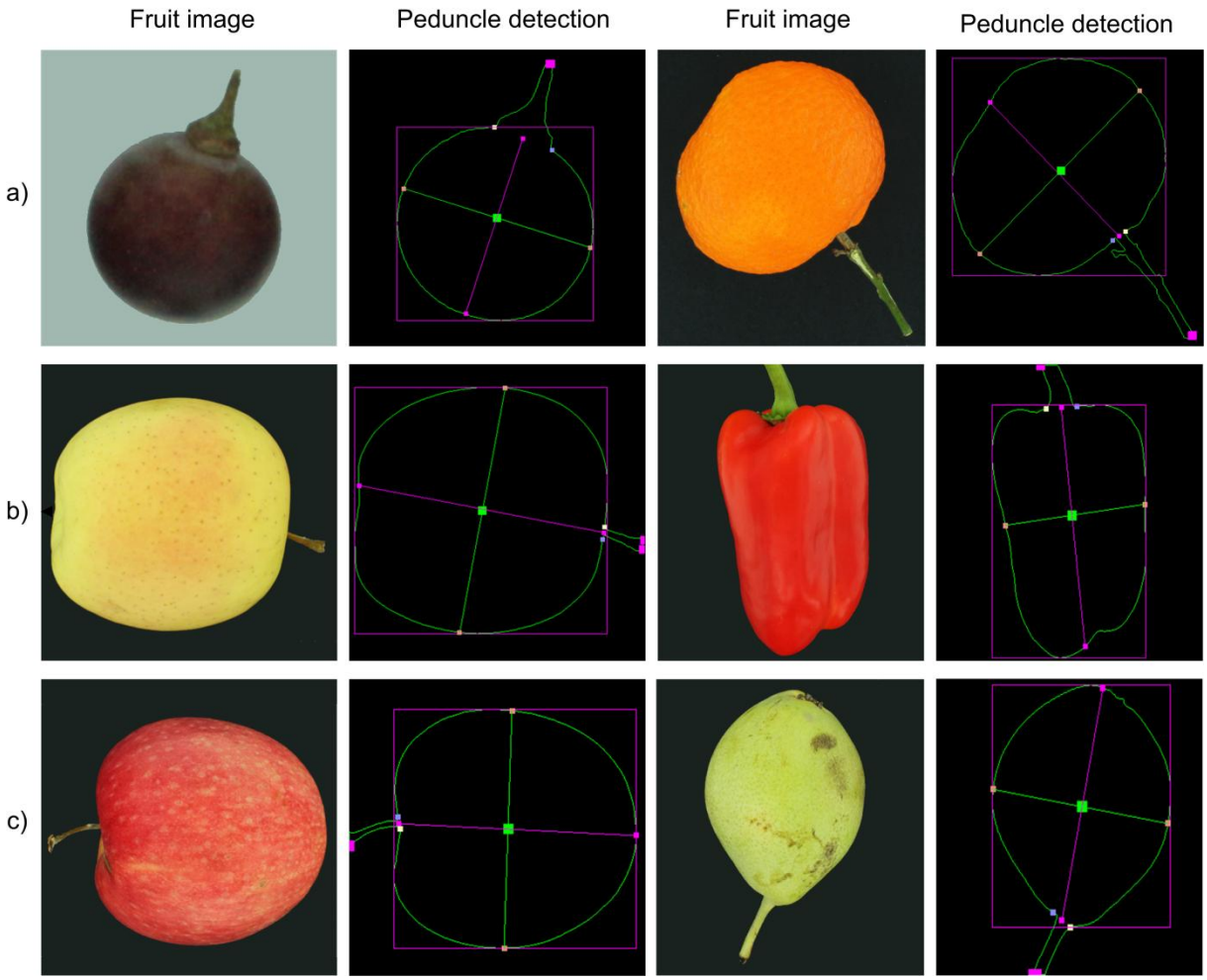

FIGURE 5. Results of peduncle detection and size estimation for some fruits tested with a random position of the peduncle: a) for grape berry and mandarin, b) for apple (‘Golden Delicious’) and red pepper, and c) for apple (‘Royal Gala’) and pear

When no peduncle was present, the direction radius signature did not vary from zero since changes in the direction of the radius signature were very smooth, and both axes of inertia were calculated from the contour to obtain the size features. Figure 6 shows the differences in the signals calculated in images with and without peduncle.

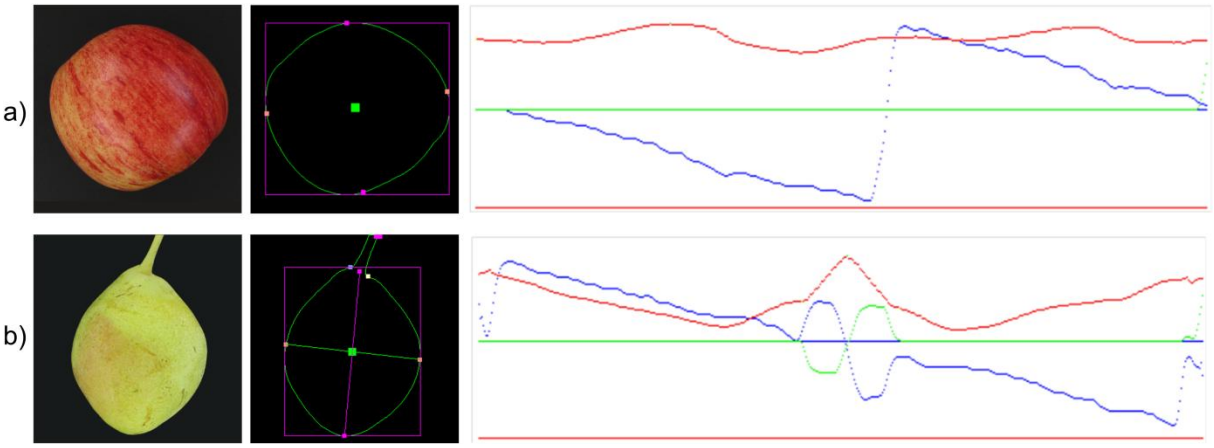

FIGURE 6. Example of results when (a) no peduncle was present in a 'Royal Gala' apple, compared to (b) a result with peduncle detected in a pear

3. Results and discussion

3.1. Assessment of grape berry size and weight by image analysis

Table 1 shows the statistical parameters for the regression model for the size estimation in 'Grenache' and 'Tempranillo' grape berries. The adjusted R^2 value obtained for the two grape varieties (0.97) confirmed the goodness of the linear regression found between the real and the estimated size values, the two coefficients being statistically significant (Table 1).

TABLE 1. Regression analyses for the estimation of the size of 'Grenache' and 'Tempranillo' grape berries

Grape variety	Parameter	Estimation	Std. error	T Statistic	P-Value
Grenache	Constant	1.0436	0.2735	3.81	<0.001
	Polar Diameter	0.9045	0.0198	45.76	<0.001
Tempranillo	Constant	0.8156	0.3350	2.44	<0.019
	Polar Diameter	0.9086	0.0237	38.32	<0.001

In order to validate the models properly, the next step was to use the regression models to predict the berry size values of the validation set. Figure 7 shows the validation results for both grapevine varieties. The validated R^2 values remained almost the same (a little bit lower, as expected for very

high R^2 values), which finally gave rise to a reliable predictive model. This result indicates that the vision system developed for the estimation of the size of grape berries with pedicel was completely reliable and could be used as a useful laboratory tool replacing the very slow and tedious manual methods that are currently employed.

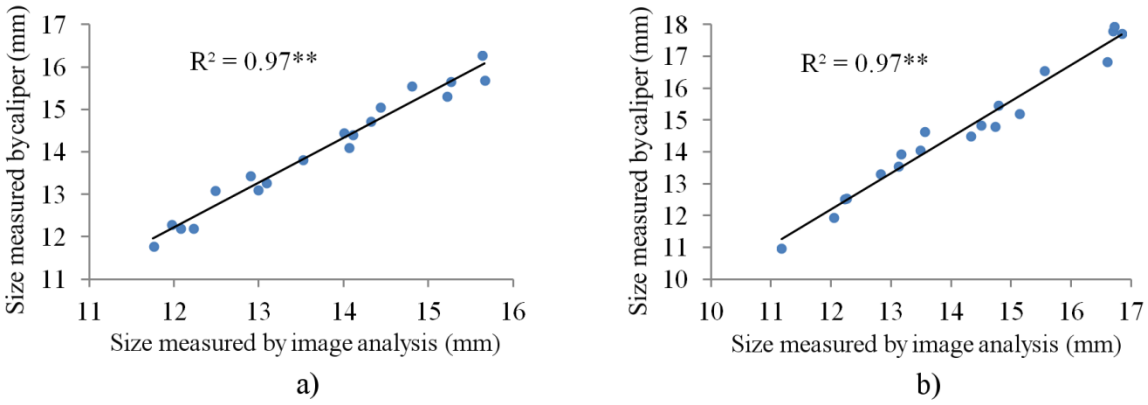

FIGURE 7. Adjustment to the linear model for the diameter of the berries from a) 'Grenache', and b) 'Tempranillo'. Statistical significance at $p<0.01$ is represented by (**)

Similar analyses were performed to assess the goodness of the system at predicting the weight of individual berries obtaining a R^2=0.98 for cv. 'Grenache' and R^2=0.96 for the cv. 'Tempranillo' (Table 2) with *P-value*<0.01 for both cultivars. To obtain more precise values of the weight, the pedicel was previously removed from the grape berries.

TABLE 2. Regression analyses for the estimation of the weight of 'Grenache' and 'Tempranillo' berries

Variety	Parameter	Estimation	Std. error	T Statistic	P-Value
Grenache	Constant	-0.6737	0.0566	-11.91	<0.001
	Weight-Area	0.0148	0.0004	38.88	<0.001
Tempranillo	Constant	-0.6593	0.0524	-12.59	<0.001
	Weight-Area	0.0149	0.0004	44.42	<0.001

To validate the models, the regression models were used to predict the weight values of the validation set. Figure 8 shows the validation results for both varieties. These results indicated that the vision system developed was also reliable for estimating the weight of grape berries of both cultivars.

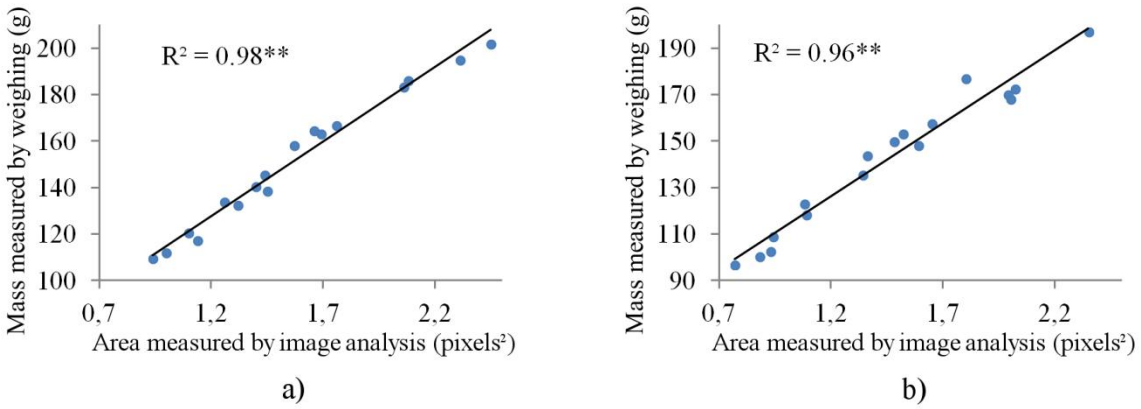

FIGURE 8. Adjustment to the linear model for the estimation of the weight of berries a) 'Grenache', and b) 'Tempranillo'. Statistical significance at $p<0.01$ is represented by (**)

Berry size and weight are common parameters for monitoring grape maturity before harvest in the wine industry (Iland et al., 2004). Nevertheless, berry weight and size determination is conducted manually in the winery laboratory, and is therefore a tedious and time-consuming task. Cluster compactness, berry colour and health grape status are properties that are strongly influenced by berry weight (Tardaguila et al., 2010) and size.

On the other hand, berry size is also related to the skin-to-pulp ratio, which is widely assumed to be a grape and wine quality factor. Since the most decisive compounds for berry and wine quality, such as aromas and phenols, are located in the skin, the larger the skin-to-pulp ratio is, the higher the potential quality of the final wine will be (Barbagallo et al., 2011). Hence, smaller berries are often considered to yield better wines and are highly appreciated by winemakers, who usually include a grape berry separation step based on their size carried out on a sorting table when the intention is to produce high-quality wines.

The methodology developed for berry weight assessment, using image analysis, is a new, fast and inexpensive tool for the wine industry to monitor berry ripening and to evaluate potential grape and

wine quality. This method could also be implemented as an inspection module on the sorting belts and tables of wineries producing high quality ultra-premium wines, thereby replacing the manual separation based on berry size that is currently performed after the de-stemming process.

3.2. Detection of peduncle in other fruits

As stated in section 2, the algorithm developed was also tested on other fruits, such as apples, pears, mandarins and peppers so as to be able to generalise it. The two functions and the signature described in section 2.3 were used to detect the peduncle, and the best results were obtained for the new radius direction signature (Table 3), which includes the correct determination of all fruits without peduncle. The main drawback of using the radius signature was that minimum values did not always match the contact points of the peduncle with the fruit when this was non-spherical (because there were points closer to the centroid than the peduncle points). Furthermore, in irregular fruits the arc-length versus turning angle function showed sudden changes in different parts of the signal, which caused confusion with the peduncle.

Regarding the estimation of the fruit size, the peduncle/pedicel axis was compared to the manual calliper measurement, an adjusted R^2>0.93 being obtained for all types of fruit. This result confirmed the goodness of the regression, since *P-value*<0.01 in all cases, thus demonstrating the reliability of the algorithms that were developed.

TABLE 3. Percentage of pedicel (grape berries) and peduncle (other fruits) detection using different signatures. For the coefficient of determination, R^2 was tested at p<0.01

Fruit	Radius function	Arc-length vs. turning angle function	Radius direction signature	Size (R^2)
Grape berry	57.0%	72.0%	100%	0.97
Mandarin	60.0%	76.7%	100%	0.97
Apple Golden Delicious	50.0%	63.3%	96.7%	0.96
Apple Royal Gala	40.0%	60.0%	96.7%	0.96
Pear	16.7%	60.0%	96.7%	0.96

Red pepper	20.0%	30.0%	90.0%	0.93

The limitations of the method mainly concerned the shape of the object, since the algorithm was able to determine the presence of the peduncle in regular and more or less rounded or compact fruits very well, but was not able to determine the presence or absence of the peduncle in fruits that were either elongated or that had irregular shapes, like the green peppers. This occurred because this method is based on the radius signature calculated as the distance of the contour points from the centre of mass. Therefore, although this centre was calculated from the area and not only from the contour, in elongated objects the centre of mass was biased to the peduncle (and sometimes outside the object surface), causing the local maximum of the polar signature to not always match the position of the end of the peduncle.

Another limitation concerns the requirement that the peduncle had to stand out from the contour of the object, which meant that the fruit or vegetable had to be oriented in order to image its profile, otherwise the peduncle could be detected, but not the correct size parameters. This can be observed in Figure 9, where the detection of the peduncle is performed correctly (Figure 9a), but the parameter of size is not (Figure 9b). In contrast, the method performed well for regular-shaped fruits. This is important since it could potentially be applied in industrial imaging vision systems. For instance, Lefcourt et al. (2009) found that under particular loading conditions in industrial systems, rotating apples generally moved to an orientation where the peduncle/pedicel axis was parallel to the plane of the track and perpendicular to the direction of travel. This orientation would allow this algorithm to detect the peduncle location properly and to measure the size of the fruits accurately in real time, since the processing time needed to analyse one image is less than 40 ms. On the other hand, it could also be implemented in harvesting robots to orient or guide the robotic hand, but in this case other problems related with the image segmentation could appear.

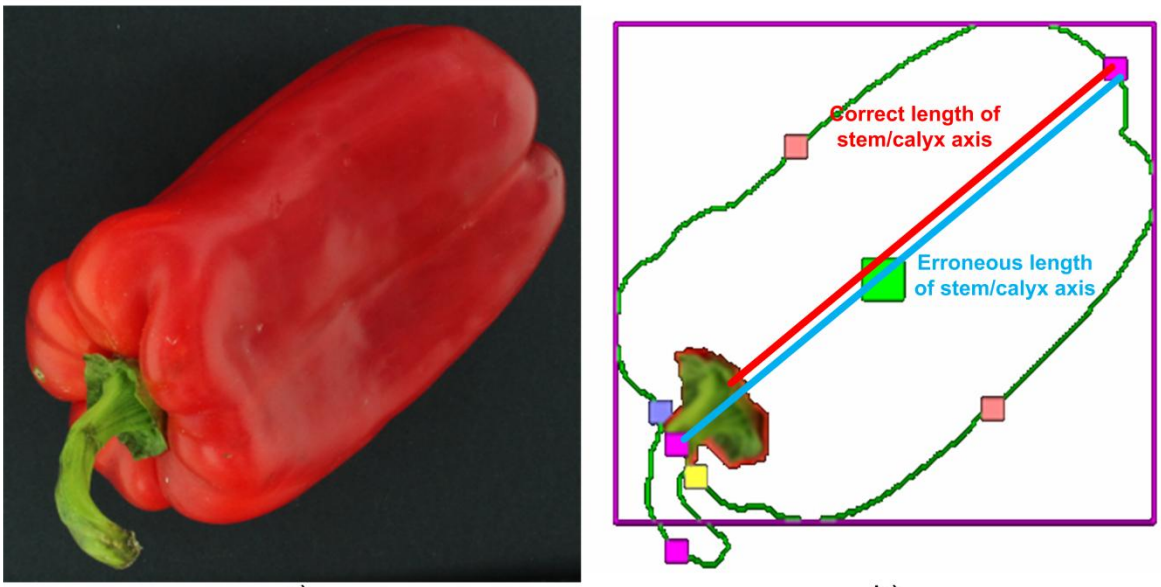

FIGURE 9. Example of result when the fruit was not well oriented on its profile and its impact on the size parameters

4. Conclusions

This work has presented a new, fast and inexpensive method to accurately assess the berry size and weight of wine-grapes, thus providing the wine industry with a cheap useful tool to monitor berry ripening and to evaluate potential grape and wine quality.

Moreover, a new effective method was developed to detect and remove the part of the peduncle/pedicel that protrudes from the fruit in the images taken by computer vision systems. The algorithm developed here could be applied to locate the peduncle/pedicel in order to have the fruit oriented or to avoid misclassification between the peduncle and defects, to accurately estimate the size while avoiding the effect of the peduncle, or also to measure the length of the peduncle. The new method does not require the segmentation of the peduncle and/or fruit defects in different regions, thereby allowing faster processing and can be used on standard images taken in the visible region of the spectrum. These two advantages make the proposed methodology faster and cheaper than other image vision methods that implement slow complex algorithms or require more expensive spectral

385 computer vision equipment. The methodology developed here may be implemented in automated
386 inspection systems and robots for multiple purposes such as sorting or harvesting tasks.

387 **Acknowledgements**

388 This work has been partially funded by the Instituto Nacional de Investigación y Tecnología Agraria y
389 Alimentaria de España (INIA) through research project RTA2012-00062-C04-01 and RTA2012-
390 00062-C04-03 with the support of European FEDER funds, by the UPV-IVIA collaboration
391 agreement through UPV-2013000005, and by UPV-SP10120276 Project.

392

393 **Reference list**

394 Barbagallo, M.G., Guidoni, S., Hunter, J.J. (2011). Berry size and qualitative characteristics of Vitis
395 vinifera L. cv. Syrah. South African Journal of Enology and Viticulture, 32, 129-136.

396 Bennedsen, B.S., Peterson D.L. (2005). Performance of a system for apple surface defect identification
397 in near-infrared images. Biosystems Engineering, 90(4), 419-431.

398 Blasco, J., Aleixos, N., Cubero, S., Gómez-Sanchis, J., Moltó, E. (2009). Automatic sorting of satsuma
399 (*Citrus unshiu)* segments using computer vision and morphological features. Computers and
400 Electronics in Agriculture, 66, 1-8.

401 Blasco, J., Aleixos, N., Gómez, J., Moltó, E. (2007). Citrus sorting by identification of the most
402 common defects using multispectral computer vision. Journal of Food Engineering, 83(3), 384-393.

403 Blasco, J., Aleixos, N., Moltó E. (2003). Machine vision system for automatic quality grading of fruit,
404 Biosystems Engineering, 85(4), 415–423.

405 Cubero, S., Aleixos, N., Moltó, E., Gómez-Sanchis, J., Blasco, J. (2011). Advances in machine vision
406 applications for automatic inspection and quality evaluation of fruits and vegetables. Food and
407 Bioprocess Technology, 4(4), 487-504.

408 Diago, M.P., Correa, C., Millan, B., Barreiro, P., Valero, C., Tardaguila, J. (2012). Grapevine yield
409 and leaf area estimation using supervised classification methodology on RGB images taken under field
410 conditions. Sensors, 12, 16988-17006.

ElMasry, G., Cubero, S., Moltó, E., Blasco, J. (2012). In-line sorting of irregular potatoes by using automated computer-based machine vision system. Journal of Food Engineering, 112, 60-68.

Freeman, H. (1961). On the encoding of arbitrary geometric configurations. IRE Transactions of Electronic Computers. EC-10, 260–268.

Guliato, D., de Carvalho, J.D., Rangayyan, R.M., Santiago, S.A. (2008). Feature extraction from a signature based on the turning angle function for the classification of breast tumors. Journal of Digital Imaging, 21(2), 129–144.

Harrel, R. C. (1991). Processing of colour images with Bayesian discriminate analysis. International Seminar on Use of Machine Vision Systems for the Agricultural and Bio-Industries, Montpellier, France, pp 11–20.

Hayashi, S., Shigematsu, K., Yamamoto, S., Kobayashi, K., Kohno, Y., Kamata, J., Kurita, M. (2010). Evaluation of a strawberry-harvesting robot in a field test. Biosystems Engineering, 105(2), 160-171.

Hayashi, S., Takahashi, K. Yamamoto, S., Saito, S., Komeda, T. (2011). Gentle handling of strawberries using a suction device. Biosystems Engineering, 109(4), 348-356.

Iland, P., Bruer, N., Edwards, G., Weeks, S., Wilkes, E. (2004). Chemical analysis of grapes and wine: techniques and concepts. Patrick Iland Wine Promotions Pty Ltd. Adelaide, Australia.

Kalvin, A., Schonberg, E., Schwartz, J.T., Sharir M. (1986). Two-dimensional, model-based, boundary matching using footprints, International Journal of Robotics Research, 5(4), 38-55.

Kapach, K., Barnea, E., Mairon, R., Edan, Y., Ben-Shahar, O. (2012). Computer Vision for Fruit Harvesting Robots - State of the Art and Challenges Ahead. Int. J. of Computational Vision and Robotics, 3(1/2), 4-34.

Kennedy, J.A. (2010). Wine colour. Understanding and managing wine quality and safety. Ed. A.G. Reynolds pp. 73-104. Woodhead Publishing. Cambridge, United Kingdom.

Kunttu, I., Lepisto, L. (2007). Shape-based retrieval of industrial surface defects using angular radius Fourier descriptor. IET Image Processing 1(2), 231–236.

436 Laykin, S., Alchanatis, V., Fallik, E., Edan Y. (2002). Image processing, machine vision, tomatoes,
437 classification. Transactions of the ASABE. 45(3), 851–858.

438 Lefcourt, A.M., Narayanan, P., Tasch, U., Kim, M.S., Reese, D., Rostamian, R., Lo, Y.M. (2009).
439 Orienting apples for imaging using their inertial properties and random apple loading. Biosystems
440 Engineering, 104(1), 64–71.

441 Lorente, D., Aleixos, N., Gómez-Sanchis, J., Cubero, S., García-Navarrete, O.L., Blasco, J. (2012).
442 Recent advances and applications of hyperspectral imaging for fruit and vegetable quality assessment.
443 Food and Bioprocess Technology, 5(4), 1121-1142.

444 Lu, R., Peng, Y. (2006) Hyperspectral scattering for assessing peach fruit firmness. Biosystems
445 Engineering, 93(2), 161-171.

446 Matthews, M.A., Nuzzo, V. (2007). Berry size and yield paradigms on grapes and wine quality. Acta
447 Horticulturae, 754, 423-436.

448 Nanyam, Y., Choudhary, R., Gupta, L., Paliwal J. (2012). A decision-fusion strategy for fruit quality
449 inspection using hyperspectral imaging. Biosystems Engineering, 111(1), 118–125.

450 Roby, G., Harbertson, J.F., Adams, D.A., Matthews, M.A. (2004). Berry size and vine water deficits
451 as factors in winegrape composition: Anthocyanins and tannins. Australian Journal of Grape and Wine
452 Research, 10, 100-107.

453 Rubine, D. (1991). Specifying gestures by example. Computer Graphics, 25 (4), 329-337.

454 Shih, F.Y. (2010). Image processing and pattern recognition: fundamentals and techniques. John
455 Wiley and Sons, New Jersy, USA

456 Tardaguila, J., Martinez de Toda, F., Poni, S., Diago, M.P. (2010). Impact of early leaf removal on
457 yield and fruit and wine composition of *Vitis vinifera* L. Graciano and Carignan. American Journal of
458 Enology and Viticulture, 61, 372-381.

459 Throop, J.A., Aneshansley, D.J., Anger, W.C., Peterson, D.L. (2003). Conveyor design for apple
460 orientation. ASAE Paper No. 03-6123.

461 Van Henten, E.J., Van Tuijl, B.A.J., Hoogakker, G.-J., Van Der Weerd, M.J., Hemming, J., Kornet,
462 J.G., Bontsema J. (2006). An autonomous robot for de-leafing cucumber plants grown in a high-wire
463 cultivation system. Biosystems Engineering, 94(3), 317–323.

464 Walker, R.R., Blackmore, D.H., Clingeleffer, P.R., Kerridge, G.H., Ruhl, E.H., Nicholas, P.R. (2005).
465 Shiraz berry size in relation to seed number and implications for juice and wine composition.
466 Australian Journal of Grape and Wine Research, 11, 2-8.

467 Wolfson, H.J. (1990). On curve matching. IEEE Transactions on Pattern Analysis and Machine
468 Intelligence, 12(5), 483-489.

469 Xing, J., Jancsók, P., De Baerdemaeker J. (2007). Stem-end/calyx identification on apples using
470 contour analysis in multispectral images. Biosystems Engineering, 96(2), 231–237.

471